Very narrow-band ultraviolet photodetection based on strained *M*-plane GaN films

Sandip Ghosh[a)]
Department of Condensed Matter Physics and Material Science, Tata Institute of Fundamental Research, Homi Bhabha Road, Mumbai 400005, India

C. Rivera, J. L. Pau, and E. Muñoz
ISOM and Departamento de Ingenierma Electrsnica, ETSI Telecomunicacisn, Universidad Politicnica de Madrid, Ciudad Universitaria, 28040 Madrid, Spain

O. Brandt and H. T. Grahn
Paul-Drude-Institut fur Festkörperelektronik, Hausvogteiplatz 5-7, 10117 Berlin, Germany

(Received 22 December 2006; accepted 26 January 2007; published online 1 March 2007)

The authors demonstrate a photodetection configuration where the responsivity in the ultraviolet spectral region is limited to a few nanometers, representing high-quality-factor, narrow-band detection together with polarization sensitivity. Both features are obtained by utilizing a polarization-sensitive photodectector in combination with a polarization filter made from two identical *M*-plane GaN films on γ-$LiAlO_2$ (100) substrate. The optical band gap of these films depends on the direction of the in-plane polarization vector of the incident light beam with respect to the *c* axis. Electronic-band-structure calculations show that the naturally present anisotropic in-plane strain in these films is the crucial parameter to achieve both a high responsivity and a high polarization contrast. © *2007 American Institute of Physics*. [DOI: 10.1063/1.2710769]

Group-III nitride semiconductors of the wurtzite crystal structure are increasingly used as ultraviolet (UV) photodetectors for applications[1–6] such as solar blind detection, UV radiation dosimetry, combustion control, flame sensors, atmospheric ozone and pollution detection, data storage, and very recently, polarization-sensitive detection.[7,8] In the area of biophotonics, the suitability of group-III nitride-based devices is being studied for real-time, laser-induced fluorescence detection of hazardous airborne biological and chemical agents.[9] For a rapid identification of a range of such chemical species, it is necessary to be able to simultaneously detect radiation emitted at specific wavelengths. This requires a set of photodetectors with very narrow-band spectral responsivity. The use of bandpass interference filters exhibiting a high quality factor in combination with a broadband detector is not ideal because of the usually poor UV transmission of typical dielectric coatings. The most common way to fabricate semiconductor UV photodetectors that operate only within a limited wavelength range is to integrate a passive filter layer into the device structure during growth. The filter layer has a larger band gap than the active region and absorbs the short-wavelength radiation, thereby limiting the short-wavelength responsivity, while the long-wavelength limit is determined by the band gap of the active region. For example, combinations consisting of $Al_{x_1}Ga_{1-x_1}N$ as the active region and $Al_{x_2}Ga_{1-x_2}N$ as the filter ($x_2 > x_1$) have been demonstrated with bandwidths ranging from 55 nm (Ref. 10) to 30 nm.[11] To achieve a bandwidth of 6 nm in the vicinity of 360 nm, this procedure would require very precisely controlled growth of layers with $x_1=0.00$ and $x_2=0.03$.

Here, we propose and demonstrate a different approach to achieve very narrow-band detection, which is based on GaN films of nonpolar orientation such as *M*-plane or *A*-plane films [see inset in Fig. 1(a)]. In such films, the effective optical band gap depends on the state of linear polarization of the incident light relative to the *c* axis, which lies in the film plane. Unlike the bandwidth-limited photodetectors described above, which are fabricated using *C*-plane films, our approach results in a detection system which is also sensitive to the state of polarization of the incident light. This added functionality may be helpful for a further reduction in spurious background signals and can yield more information in suitably designed applications.[12] Finally, we discuss how the in-plane strain in these films affects the performance of our narrow-band detection configuration (NBDC).

The 0.4 μm thick, $[1\bar{1}00]$ oriented *M*-plane GaN film was grown on a γ-$LiAlO_2$ (100) substrate using rf plasma-assisted molecular-beam epitaxy.[13] Its orientation and single-phase nature were verified using high-resolution x-ray diffraction (HRXRD) measurements, which also demonstrated that the film is under an overall compressive in-plane strain with an out-of-plane dilation $\epsilon_{yy}=0.39\%$. The in-plane strain is anisotropic, i.e., $\epsilon_{xx} \neq \epsilon_{zz}$. It is mainly determined by the lattice mismatch between the film and substrate but also depends on the difference in their thermal expansion coefficients along directions parallel and perpendicular to the *c* axis. By changing the film thickness, the in-plane strain can be varied within a certain range. Planar Schottky barrier photodetectors of circular geometry were fabricated from one piece of the wafer, while a polarization filter was taken from another piece of the same wafer. The active region of the photodetector with a radius of 200 μm has a semitransparent, rectifying Au (12 nm thick) contact with a surrounding Ohmic contact of Ti (50 nm)/Al (200 nm).[8] The optical measurements were performed using a 75 W Xe lamp and a reflection-grating-based monochromator. The light was po-

[a)]Electronic mail: sangho10@tifr.res.in

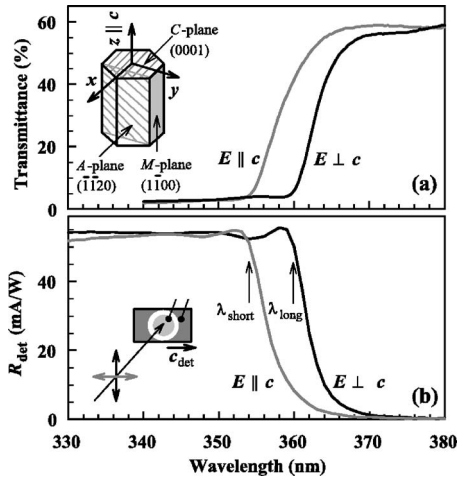

FIG. 1. (a) Transmission spectrum of the *M*-plane GaN film for $\boldsymbol{E}\|\boldsymbol{c}$ and $\boldsymbol{E}\perp\boldsymbol{c}$ at 297 K. The inset shows the unit cell of wurtzite GaN and the choice of coordinates. (b) Spectral responsivity R_{det} of a Schottky diode photodetector processed from the *M*-plane film for $\boldsymbol{E}\|\boldsymbol{c}$ and $\boldsymbol{E}\perp\boldsymbol{c}$. The inset depicts a schematic of the device and the measurement geometry.

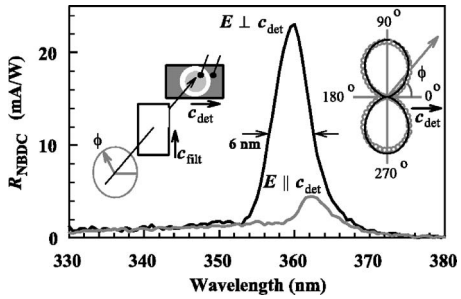

FIG. 2. Spectral responsivity R_{NBDC} of the NBDC for $\boldsymbol{E}\|\boldsymbol{c}_{\mathrm{det}}$ and $\boldsymbol{E}\perp\boldsymbol{c}_{\mathrm{det}}$ at 297 K. The left inset displays the measurement configuration. The right inset depicts a polar plot of the measured relative R_{NBDC} at 360 nm (circles) as a function of the in-plane polarization angle ϕ, the line represents a fit to $R_{\mathrm{NBDC}}=R^{\max}\sin^2(\phi)$.

larized using Glan-Taylor polarizers. The responsivity was calibrated by comparison with a standard UV-enhanced Si photodiode.

Figure 1(a) shows the transmission spectrum of the *M*-plane film for normally incident light with the electric field vector $\boldsymbol{E}$ being polarized perpendicular ($\boldsymbol{E}\perp\boldsymbol{c}$) and parallel ($\boldsymbol{E}\|\boldsymbol{c}$) to the *c* axis. The shift in the transmission edge is due to the difference in the optical band gap for the two polarizations. This in turn leads to a polarization-dependent spectral shift in the responsivity (R_{det}) of the Schottky barrier photodetector fabricated from this film as shown in Fig. 1(b). The wavelength λ_{short} (λ_{long}) corresponds to the effective excitonic band gap for $\boldsymbol{E}\|\boldsymbol{c}$ ($\boldsymbol{E}\perp\boldsymbol{c}$). Note that the responsivity remains high at shorter wavelengths. In order to achieve a narrow-band spectral responsivity, we use another piece of the as-grown *M*-plane film as a filter, placing it in front of the photodetector such that $\boldsymbol{c}_{\mathrm{filt}}$ is perpendicular to $\boldsymbol{c}_{\mathrm{det}}$ (see left inset in Fig. 2). This combination of detector and filter operates in the following way. For $\boldsymbol{E}\|\boldsymbol{c}_{\mathrm{det}}$, light with $\lambda\leqslant\lambda_{\mathrm{short}}$ is absorbed by the filter and consequently prevented from reaching the photodetector, while light with $\lambda_{\mathrm{short}}\leqslant\lambda\leqslant\lambda_{\mathrm{long}}$ is transmitted by the filter and can therefore reach the detector. In contrast, all light with $\lambda\leqslant\lambda_{\mathrm{long}}$ will be absorbed by the filter for $\boldsymbol{E}\|\boldsymbol{c}_{\mathrm{det}}$ so that no light of this polarization will be detected. The presence of the small signal for $\boldsymbol{E}\|\boldsymbol{c}_{\mathrm{det}}$ is essentially due to absorption at energies below the band gap,[14] which reduces the anisotropy. Thus, the NBDC detects light of polarization $\boldsymbol{E}\perp\boldsymbol{c}_{\mathrm{det}}$ in the wavelength band $\Delta\lambda=\lambda_{\mathrm{long}}-\lambda_{\mathrm{short}}$ as shown in Fig. 2. In the present case, the responsivity peaks at 360 nm with a bandwidth of $\Delta\lambda=6$ nm. The measured dependence of the NBDC responsivity (R_{NBDC}) at 360 nm on the in-plane polarization angle ϕ, which is defined relative to $\boldsymbol{c}_{\mathrm{det}}$, is well described by $R_{\mathrm{NBDC}}=R^{\max}\sin^2(\phi)$ (see right inset in Fig. 2). For this type of NBDC, one could also use *A*-plane GaN films grown on *R*-plane sapphire or *A*-plane SiC.[15,16] However, only the substrates $LiAlO_2$ and sapphire are transparent down to 200 nm, thus facilitating operation in the UV spectral range.

The performance of the NBDC will depend on the polarization properties and energies of the three optical transitions in the vicinity of the band gap of GaN. These transitions occur from the three top valence bands (VBs), whose wave functions have a mixture of atomic p_x, p_y, and p_z orbital character, to the conduction band, which has *s* character. The transitions from p_x, p_y, and p_z symmetry to *s* symmetry require $\boldsymbol{x}$, $\boldsymbol{y}$, and $\boldsymbol{z}$ polarized light, respectively. Since these transitions are highly sensitive to any strain in the film, we have used the Bir-Pikus Hamiltonian[17] to calculate its influence on the electronic band structure (EBS). The energy splitting and deformation potential parameters used are based on recent results[16,18] on unstrained *C*-plane and anisotropically strained *M*- and *A*-plane GaN films, respectively, while the elastic constants are taken from Ref. 19. The values of all these parameters are listed in Ref. 20. We use the nomenclature T_i $(i=1,2,3)$ for the three transitions in order of decreasing transition edge wavelengths $\lambda_{T_1}>\lambda_{T_2}>\lambda_{T_3}$ for any values of ϵ_{xx} and ϵ_{zz}. The relative oscillator strengths of T_i are labeled $f_{i\beta}$, where $\beta=x,y,z$ represents the polarization components. The strain mixes the VBs and can result in dramatic modifications of $f_{i\beta}$ so that the transitions can become completely linearly polarized along $\boldsymbol{x}$, $\boldsymbol{y}$, and $\boldsymbol{z}$.[17]

For efficient operation of the NBDC, high absorption is necessary for one polarization direction (e.g., $\boldsymbol{E}\perp\boldsymbol{c}$), while no absorption should occur for the orthogonal polarization (e.g., $\boldsymbol{E}\|\boldsymbol{c}$) in the wavelength range λ_{long} to λ_{short}. Next, for $\lambda<\lambda_{\mathrm{short}}$, we need a high absorption for the orthogonal polarization ($\boldsymbol{E}\|\boldsymbol{c}$) so that the filter efficiently blocks such light from reaching the detector. The above considerations imply that, if λ_{long} (λ_{short}) is associated with T_1 (T_2), the oscillator strengths must be such that the quantity $[f_{1x}-f_{1z}]f_{2z}$ or $[f_{1z}-f_{1x}]f_{2x}$ is positive and maximal. In the former (latter) case, the polarization $\boldsymbol{E}\perp\boldsymbol{c}_{\mathrm{det}}$ ($\boldsymbol{E}\|\boldsymbol{c}_{\mathrm{det}}$) will be detected. Due to absorption of light below the band gap,[14] the central operating wavelength λ_c of the NBDC is likely to be closer to λ_{long}. The graphs in Figs. 3(a) and 3(b) depict the dependence of the above quantities on ϵ_{xx} and ϵ_{zz}. The dark regions, which essentially occur for overall compressive in-plane strain, identify the strain values which are best suited for the operation of the NBDC. The corresponding $\Delta\lambda$ and $\lambda_c=\lambda_{T_1}$ are plotted in Figs. 3(c) and 3(d). If T_1 is completely *y* polarized, one can associate λ_{long} (λ_{short}) with T_2 (T_3). In this case, we need positive maximal values for $f_{1y}[f_{2x}-f_{2z}]f_{3z}$ or $f_{1y}[f_{2z}-f_{2x}]f_{3x}$, which occur for overall tensile in-plane strain as shown in Figs. 3(e) and 3(f). The corresponding $\Delta\lambda$ and $\lambda_c=\lambda_{T_2}$ are plotted in Figs. 3(g) and 3(h). These results demonstrate that both an anisotropic compressive and an anisotropic tensile in-plane strain are desirable

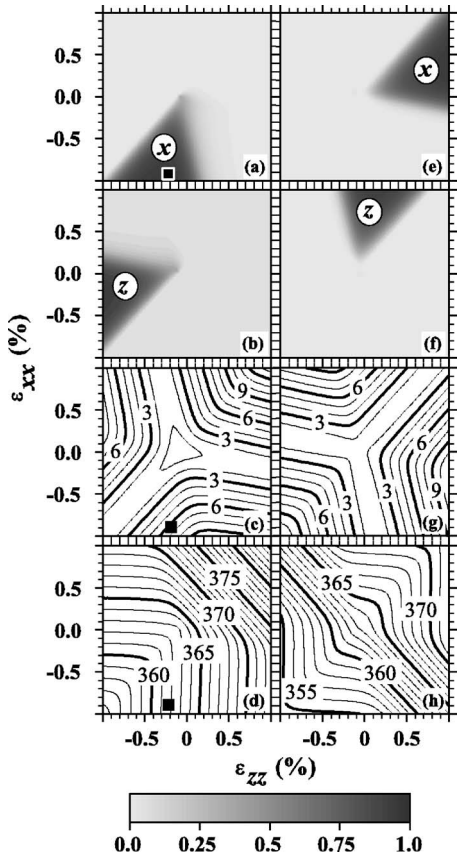

FIG. 3. (a) Positive values of $[f_{1x}-f_{1z}]f_{2z}$ and (b) $[f_{1z}-f_{1x}]f_{2x}$ as a function of in-plane strain in an *M*-plane GaN film. The dark regions indicate strain values favorable for NBDC involving the transitions T_1 and T_2. The label *x* (*z*) indicates that the polarization $\boldsymbol{E}\perp\boldsymbol{c}_{\mathrm{det}}$ ($\boldsymbol{E}\|\boldsymbol{c}_{\mathrm{det}}$) will be detected. (c) Detection bandwidth $\Delta\lambda$ and (d) central operating wavelength λ_c in nanometers for detection involving T_1 and T_2 [(a) and (b)]. Black squares mark the in-plane strain determined for the investigated *M*-plane GaN film. (e) Positive values of $f_{1y}[f_{2x}-f_{2z}]f_{3z}$ and (f) $f_{1y}[f_{2z}-f_{2x}]f_{3x}$ for detection involving T_2 and T_3. (g) $\Delta\lambda$ and (h) λ_c in nanometers for detection involving T_2 and T_3 [(e) and (f)].

for the operation of the NBDC, and a minimum bandwidth of $\Delta\lambda=3$ nm with high responsivity and polarization contrast can be achieved for compressive in-plane strain. We have ignored the combination T_1 and T_3, when T_2 is completely *y* polarized, since it results in a larger $\Delta\lambda$.

Comparing the HRXRD and optical spectroscopy data with the results of the EBS calculations, we can assign the transition edge in our film for $\boldsymbol{E}\perp\boldsymbol{c}$ ($\boldsymbol{E}\|\boldsymbol{c}$) to T_1 (T_2) and estimate the in-plane strain to be $\epsilon_{xx}\approx-0.9\%$ and $\epsilon_{zz}\approx-0.22\%$. These values fall in the dark region of Fig. 3(a) (marked by a square). The corresponding calculated values of $\Delta\lambda=6$ nm and $\lambda_c=361.5$ nm agree fairly well with the measured values for the NBDC. Note that a 1 μm thick *M*-plane film on γ-$LiAlO_2$ typically has in-plane strain[17] corresponding to the dark region of Fig. 3(a). The utilization of thicker films in the NBDC can further improve the rejection at $\lambda<\lambda_{\mathrm{short}}$ by a factor larger than 250. Due to the symmetry of the wurtzite crystal structure, these results are also valid for anisotropic strain in *A*-plane GaN films with *x* and *y* interchanged everywhere.[15] For a shorter (longer) λ_c, one can use suitable $Al_xGa_{1-x}N$ ($In_xGa_{1-x}N$) alloy compositions, for which similar calculations are necessary to determine the strain required for optimal performance.

In conclusion, we have proposed and demonstrated very narrow-band photodetection in the UV spectral range using wurtzite group-III nitride films of nonpolar orientation, which in addition to its narrow-band spectral responsivity is also polarization sensitive. The anisotropic in-plane strain, which is naturally present in such films, is essential for the efficient operation of such a detection system. This configuration, when used specifically for polarization sensing, may perform better than the bare polarization-sensitive photodetector[8] because the limited spectral bandwidth ensures a lower spurious background signal.

One of the authors (S.G.) acknowledges useful discussions with Jayeeta Bhattacharyya.

[1] M. Razeghi and A. Rogalski, J. Appl. Phys. **79**, 7433 (1996).
[2] G. Parish, S. Keller, P. Kozodoy, J. P. Ibbetson, H. Marchand, P. T. Fini, S. B. Fleischer, S. P. DenBaars, U. K. Mishra, and E. J. Tarsa, Appl. Phys. Lett. **75**, 247 (1999).
[3] E. Muñoz, E. Monroy, F. Calle, F. Omnès, and P. Gibart, J. Geophys. Res. **105**, 4865 (2000).
[4] J. L. Pau, J. Anduaga, C. Rivera, Á. Navarro, I. Álava, M. Redondo, and E. Muñoz, Appl. Opt. **45**, 7498 (2006).
[5] T. Li, J. H. Lambert, A. L. Beck, C. J. Collins, B. Yang, M. M. Wong, U. Chowdhury, R. D. Dupuis, and J. C. Campbell, J. Electron. Mater. **30**, 872 (2001).
[6] M. A. Khan, M. Shatalov, H. P. Maruska, H. M. Wang, and E. Kuokstis, Jpn. J. Appl. Phys., Part 1 **44**, 7191 (2005).
[7] S. Ghosh, O. Brandt, H. T. Grahn, and K. H. Ploog, Appl. Phys. Lett. **81**, 3380 (2002).
[8] C. Rivera, J. L. Pau, E. Muñoz, P. Misra, O. Brandt, H. T. Grahn, and K. H. Ploog, Appl. Phys. Lett. **88**, 213507 (2006).
[9] G. A. Wilson and R. K. DeFreez, Proc. SPIE **5416**, 157 (2004).
[10] S. K. Zhang, W. B. Wang, F. Yun, L. He, H. Morkoç, X. Zhou, M. Tamargo, and R. R. Alfano, Appl. Phys. Lett. **81**, 4628 (2002).
[11] U. Karrer, A. Dobner, O. Ambacher, and M. Stutzmann, J. Vac. Sci. Technol. B **18**, 757 (2000).
[12] S. Umeyama and G. Godin, IEEE Trans. Pattern Anal. Mach. Intell. **26**, 639 (2004).
[13] P. Waltereit, O. Brandt, M. Ramsteiner, R. Uecker, P. Reiche, and K. H. Ploog, J. Cryst. Growth **218**, 143 (2000).
[14] V. Lebedev, I. Cimalla, U. Kaiser, and O. Ambacher, Phys. Status Solidi C **1**, 233 (2004).
[15] S. Ghosh, P. Misra, H. T. Grahn, B. Imer, S. Nakamura, S. P. DenBaars, and J. S. Speck, J. Appl. Phys. **98**, 026105 (2005).
[16] P. Misra, U. Behn, O. Brandt, H. T. Grahn, B. Imer, S. Nakamura, S. P. DenBaars, and J. S. Speck, Appl. Phys. Lett. **88**, 161920 (2006).
[17] S. Ghosh, P. Waltereit, O. Brandt, H. T. Grahn, and K. H. Ploog, Phys. Rev. B **65**, 075202 (2002).
[18] U. Behn, P. Misra, H. T. Grahn, B. Imer, S. Nakamura, S. P. DenBaars, and J. S. Speck, Phys. Status Solidi A **204**, 299 (2007).
[19] I. Vurgaftman and J. R. Meyer, J. Appl. Phys. **94**, 3675 (2003).
[20] The deformation potentials are $\alpha_{\mathrm{CB}}=-44.5$ eV, $D_1=-41.4$ eV, $D_2=-33.3$ eV, and $D_5=-3.6$ eV. The crystal-field and spin-orbit splitting energies are $\Delta_{\mathrm{cr}}=\Delta_1=9.2$ meV and $\Delta_{\mathrm{so}}=3\Delta_2=18.9$ meV. The other parameters are obtained under the quasicubic approximation. The exciton binding energies are taken to be 26 meV. The wavelength of the unstrained *A*-exciton transition is taken to be 363.6 nm at 297 K. The elastic constants are $C_{11}=390$ GPa, $C_{12}=145$ GPa, $C_{13}=106$ GPa, and $C_{33}=398$ GPa.